


**VASCULAR BIOLOGY, ATHEROSCLEROSIS, AND ENDOTHELIUM BIOLOGY**

# 7-Ketocholesterol Induces Autophagy in Vascular Smooth Muscle Cells through Nox4 and Atg4B

Chaoyong He,<sup>\*</sup> Huaiping Zhu,<sup>\*</sup> Wencheng Zhang,<sup>\*</sup> Imoh Okon,<sup>\*</sup> Qilong Wang,<sup>\*</sup> Hongliang Li,<sup>\*</sup> Yun-Zheng Le,<sup>†‡§</sup> and Zhonglin Xie<sup>\*</sup>

From the Sections of Molecular Medicine<sup>\*</sup> and Endocrinology and Diabetes,<sup>†</sup> Department of Medicine, the Department of Cell Biology,<sup>‡</sup> and the Harold Hamm Oklahoma Diabetes Center,<sup>§</sup> University of Oklahoma Health Sciences Center, Oklahoma City, Oklahoma

Accepted for publication  
 April 16, 2013.

Address correspondence to  
 Zhonglin Xie, M.D., Ph.D.,  
 Section of Molecular Medicine,  
 Department of Medicine,  
 University of Oklahoma Health  
 Sciences Center, 941 Stanton L.  
 Young Blvd., BSEB 302B,  
 Oklahoma City, OK 73104.  
 E-mail: [zxie@ouhsc.edu](mailto:zxie@ouhsc.edu).

Oxidized lipoproteins stimulate autophagy in advanced atherosclerotic plaques. However, the mechanisms underlying autophagy induction and the role of autophagy in atherogenesis remain to be determined. This study was designed to investigate the mechanisms by which 7-ketocholesterol (7-KC), a major component of oxidized lipoproteins, induces autophagy. This study was also designed to determine the effect of autophagy induction on apoptosis, a central event in the development of atherosclerosis. Exposure of human aortic smooth muscle cells to 7-KC increased autophagic flux. Autophagy induction was suppressed by treating the cells with either a reactive oxygen species scavenger or an antioxidant. Administration of 7-KC concomitantly up-regulated Nox4 expression, increased intracellular hydrogen peroxide levels, and inhibited autophagy-related gene 4B activity. Catalase overexpression to remove hydrogen peroxide or Nox4 knockdown with siRNA reduced intracellular hydrogen peroxide levels, restored autophagy-related gene 4B activity, and consequently attenuated 7-KC-induced autophagy. Moreover, inhibition of autophagy aggravated both endoplasmic reticulum (ER) stress and cell death in response to 7-KC. In contrast, up-regulation of autophagic activity by rapamycin had opposite effects. Finally, activation of autophagy by chronic rapamycin treatment attenuated ER stress, apoptosis, and atherosclerosis in apolipoprotein E knockout (*ApoE*<sup>-/-</sup>) mouse aortas. In conclusion, we demonstrate that up-regulation of autophagy is a cellular protective response that attenuates 7-KC-induced cell death in human aortic smooth muscle cells. (*Am J Pathol* 2013, 183: 626–637; <http://dx.doi.org/10.1016/j.ajpath.2013.04.028>)

Autophagy is a highly conserved cellular process for degradation of cytoplasmic components, such as long-lived proteins and damaged organelles in lysosomes.<sup>1</sup> The process is essential for the maintenance of cellular homeostasis and survival because the degradation of cytosolic components can provide amino acids and substrates for intermediary metabolism.<sup>2</sup> Although dysregulation of autophagy has been implicated in many human diseases, including neurodegeneration, cancer, and cardiomyopathy,<sup>3–5</sup> little information exists about the role of autophagy in the development of atherosclerosis. Recently, oxidized lipoproteins have been demonstrated to stimulate autophagy in advanced atherosclerotic plaques,<sup>6</sup> leading us to hypothesize that oxidized lipoproteins may induce autophagy in vascular cells through increasing intracellular reactive oxygen species (ROS). In support of this model, a strong correlation between oxidative

stress and the development of atherosclerosis has been established<sup>7</sup> and starvation-induced ROS have been demonstrated to trigger autophagy by oxidizing a critical cysteine residue in autophagy-related gene 4 (Atg4) protein.<sup>8</sup>

Atherosclerosis is characterized by the accumulation of oxidized lipoproteins in large arteries. Oxidation of lipoproteins leads to the formation of dozens of new lipids, such as oxysterols, aldehydes, and oxidized fatty acids.<sup>7</sup> These oxidized lipoproteins could promote the progression of atherosclerosis by stimulating an inflammatory response, increasing foam cell formation, and inducing vascular cell

Supported by NIH grant (1P20RR024215-01 to Z.X.), a Scientist Development grant from the American Heart Association (Z.X.), and an Oklahoma Center for Advancement of Science and Technology grant (Z.X.).

apoptosis.<sup>9</sup> Oxysterols, such as 7 $\beta$ -hydroxycholesterol and 7-ketocholesterol (7-KC), are major components of oxidized lipoproteins in human atherosclerotic plaques.<sup>10</sup> The oxysterol 7-KC has been shown to accelerate ROS production and induce complex modes of cell death,<sup>11</sup> including necrosis,<sup>12</sup> apoptosis (type I cell death),<sup>13</sup> and autophagic type II cell death. Martinet et al<sup>11</sup> demonstrated that 7-KC activates the ubiquitin proteasome system and induces the formation of a myelin figure and the processing of microtubule-associated protein light chain 3 (LC3). However, the molecular mechanisms by which 7-KC induces autophagy and the role of autophagy induction in the development of atherosclerosis remain undefined. Therefore, we investigated the mechanism by which 7-KC induces autophagy and the effect of autophagy on apoptosis, an important process in the development of atherosclerosis. We found that 7-KC increased Nox4-mediated hydrogen peroxide formation, which triggered autophagy through the inhibition of Atg4B activity. The induction of autophagy mitigated vascular smooth muscle cell (VSMC) death by suppressing the endoplasmic reticulum (ER) stress–apoptosis pathway.

## Materials and Methods

### Reagents

We used the following antibodies: antibodies against Beclin1, LC3B, Atg4B, and phosphorylated eukaryotic initiation factor-2  $\alpha$  (P-eIF2 $\alpha$ ) (Cell Signaling Inc., Beverly, MA), antibodies against Atg4A and 78 kDa glucose-regulated protein (GRP78) (Abcam, Cambridge, MA), antibodies against catalase and reduced nicotinamide-adenine dinucleotide phosphate (NADPH) oxidase (Nox) subunits (Nox4, catalog number sc-55142; Nox5, catalog number sc-67006) (Santa Cruz Biotechnology, Santa Cruz, CA), antibody against Nox1 (catalog number NBP1-69573; Novus Biologicals, Littleton, CO), and the antibody against activating transcription factor 6 (Imgenex, San Diego, CA). Human aortic smooth muscle cells (HASMCs) and cell culture media were purchased from Cascade Biologics (Portland, OR). The hydrogen peroxide cell-based assay kit was obtained from Cayman Chemical Company (Ann Arbor, MI). Chemicals, along with 7-KC, were obtained from Sigma-Aldrich (St. Louis, MO).

### Animals

Male apolipoprotein E knockout (*ApoE*<sup>-/-</sup>) mice used for these experiments were obtained from Jackson Laboratories (Bar Harbor, ME). Six-week-old mice that were maintained on a high fat diet (1.3% cholesterol, 0.5% cholic acid, TD 02028; Harlan Teklad, Madison, WI) were treated with or without 8 mg/kg/day, subcutaneous injection of rapamycin. After 8 weeks of treatment, aortas were isolated for immunohistochemical analysis, terminal deoxynucleotidyl transferase-mediated dUTP nick-end labeling (TUNEL), and Oil Red O

staining. All animal protocols were reviewed and approved by the University of Oklahoma Institutional Animal Care and Use Committee.

### Cell Culture and Treatments

HASMCs were maintained in Medium 231 with smooth muscle cell growth supplement. All culture media were supplemented with 100 units/mL penicillin and 100  $\mu$ g/mL streptomycin. HASMCs at passages 3 to 8 and grown to 70% to 80% confluence were used for the experiments. All cells were incubated in a humidified atmosphere of 5% CO<sub>2</sub> and 95% air at 37°C. Stock solutions of 7-KC (20 mmol/L) were freshly prepared by dissolving 7-KC in dimethyl sulfoxide. To exclude the toxic effect of dimethyl sulfoxide, control cells were treated with an equal amount of solvent.

### Adenovirus Infection

HASMCs were infected with adenovirus encoding catalase at a multiplicity of infection of 100 in medium with 5% fetal calf serum for 48 hours, and an adenovirus encoding green fluorescent protein (GFP) was used as a control. Under these conditions, infection efficiency was >80% as determined by GFP expression.<sup>14,15</sup>

### RNA Extraction and Real-Time PCR

Total mRNA was extracted from the cultured cells with Trizol reagent (Invitrogen, Grand Island, NY). For reverse transcription, 1  $\mu$ g of the total mRNA was converted to first strand complementary DNA in a 20  $\mu$ L reaction volume using a cDNA synthesis Kit (Promega, Madison, WI). Expression levels of human Nox1, Nox4, Nox5, and housekeeping  $\beta$ -actin mRNAs were determined by using the specific primer as follows: Nox1, forward 5'-GTACAAATTCCAGTGTGCA-GACCAC-3', reverse 5'-CAGACTGGAATATCGGTGACAGCA-3'; Nox4, forward 5'-CTCAGCGGAATCAATC-AGCTGTG-3', reverse 5'-AGAGGAACACGACAATCA-GCCTTAG-3'; Nox5, forward 5'-ATCAAGCGCCCCC-TTTTTTTCAC3', reverse 5'-CTCATTGTACACTCCTC-GACAGC-3'; and  $\beta$ -actin, forward 5'-GCAGCCCAGC-CAGCACTGTCAGG-3', reverse 5'-AGCCCAGAGCCATT-GTCACACACCAA-3'. Quantitative real-time-PCR reactions were performed as described.<sup>16</sup> Quantifications were performed by a comparative method (2<sup>- $\Delta\Delta$ Ct</sup>) using  $\beta$ -actin transcripts as an internal control.<sup>17</sup>

### Visualization of Autophagic Vacuoles

HASMCs were plated at 5  $\times$  10<sup>4</sup> cells per well and were allowed to adhere to the plate overnight. Cells were then transduced with LC3B-GFP using Premo autophagy sensors (LC3B-FP) from Invitrogen. After 24 hours of transfection, the cells were incubated with 5  $\mu$ mol/L of chloroquine (CQ) for 16 hours in the presence or absence of 7-KC. Fluorescence images were obtained by using an inverted

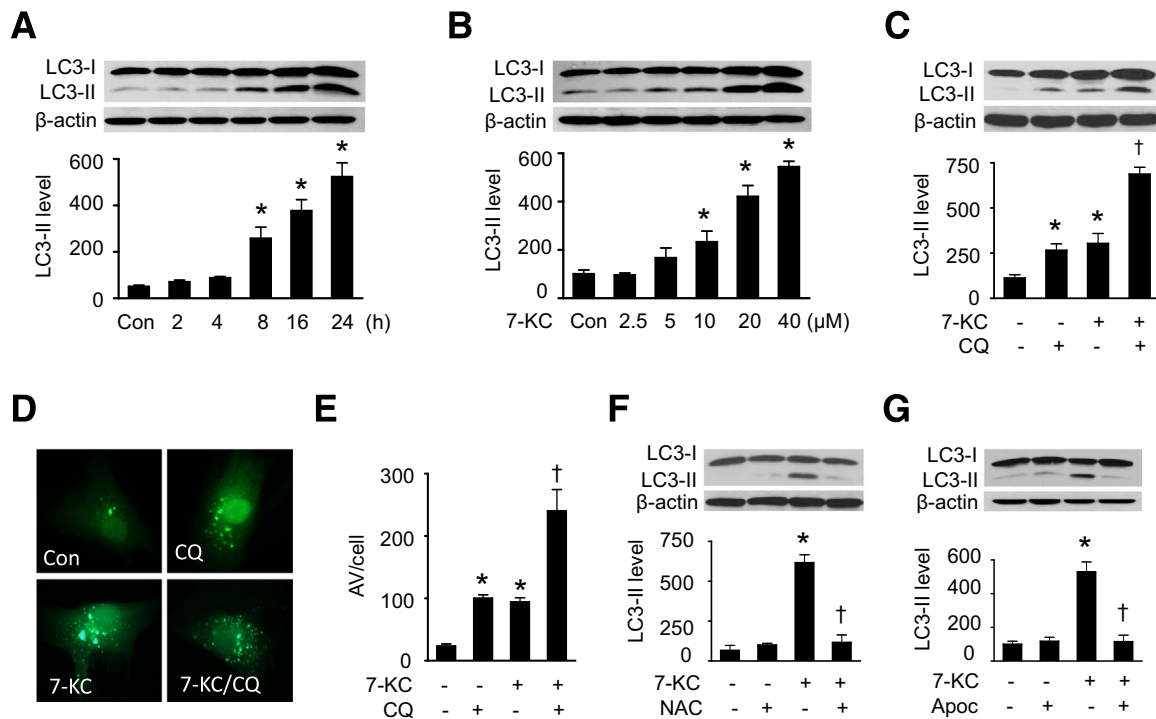


**Figure 1** 7-KC–induced autophagy is reactive oxygen species (ROS)-dependent. **A:** HASMCs were treated with 20  $\mu\text{mol/L}$  7-KC for the indicated times, and cell lysates were subjected to Western blot analysis for LC3-II protein levels ( $n = 6$ ). **B:** HASMCs were treated with indicated concentrations of 7-KC for 16 hours. LC3-II protein levels in cell lysates were detected by Western blot analysis ( $n = 6$ ). **C:** HASMCs were incubated with 20  $\mu\text{mol/L}$  7-KC for 16 hours in the presence or absence of 5  $\mu\text{mol/L}$  chloroquine (CQ). Autophagic flux was defined by the difference in LC3-II protein levels between the cells treated with and without CQ ( $n = 5$ ). **D:** HASMCs were transfected with LC3B-GFP for 24 hours, and then incubated with 5  $\mu\text{mol/L}$  CQ for 16 hours in the presence or absence of 7-KC. Fluorescence images were obtained by using an inverted fluorescent microscope. Similar results were obtained in three independent experiments. **E:** Mean number of autophagosomal vacuole (AV) per cell ( $n = 3$ ). **F:** HASMCs were pretreated with 2 mmol/L N-acetyl cysteine (NAC) for 1 hour and then treated with 20  $\mu\text{mol/L}$  7-KC for 16 hours. Expression of LC3 in cell lysates was examined by using Western blot analysis ( $n = 5$ ). **G:** HASMCs were pretreated with 300  $\mu\text{mol/L}$  apocynin (Apoc) for 1 hour, and then treated with 7-KC for 16 hours. Cell lysates were subjected to Western blot analysis for LC3-II protein levels ( $n = 5$ ). \* $P < 0.05$  versus control (Con), † $P < 0.05$  versus 7-KC.

fluorescent microscope (Olympus America, Melville, NY). Autophagy was measured by quantifying the average number of autophagosomes per cell for each sample. A minimum of 100 cells per sample was counted.<sup>18</sup>

### Gene Silencing with siRNA

Scrambled siRNA (5'-CUUACGCUGAGUACUUCGATT-3'), Beclin1 siRNA (5'-CTCAGGAGAGGAGCCATTT-3'), and Nox4 siRNA (5'-GTCAACATCCAGCTGTACC-3') were obtained from Applied Biosystems (Foster City, CA). Transfection was performed according to the manufacturer's instructions. The efficiency of siRNA-silenced genes was evaluated by Western blot analysis of the targeted proteins with specific antibodies.

### Western Blot Analysis

Western blot analysis was performed with specific antibodies. Optical density of bands was quantified by AlphaEase ( $\alpha$  Innotech Corporation, San Leandro, CA) and expressed as arbitrary units as previously described.<sup>14,19,20</sup>

### Assay of Hydrogen Peroxide

Hydrogen peroxide was detected by using the hydrogen peroxide Cell-based Assay kit (Cayman Chemical Company, Ann Arbor, MI) in which hydrogen peroxide is detected with 10-acetyl-3,7-dihydroxyphosphoxazine, a highly sensitive and stable probe for hydrogen peroxide.<sup>21</sup> Cells were grown in a 96-well plate at a density of  $6 \times 10^4$  cells per well overnight. After the treatments, hydrogen peroxide was measured according to the manufacturer's instructions.

### Cell Viability Assay

Cell viability assays were performed by using the Cell Counting kit-8 (Dojindo Molecular Technologies, Rockville, MD) according to the manufacturer's protocol. Absorbance was measured with a Bio-Rad Benchmark microplate reader (Hercules, CA) at 450 nm.

### Quantitative Detection of Cell Apoptosis

Apoptosis was analyzed by using a fluorescein isothiocyanate Annexin V Apoptosis Detection kit (BD Biosciences, San

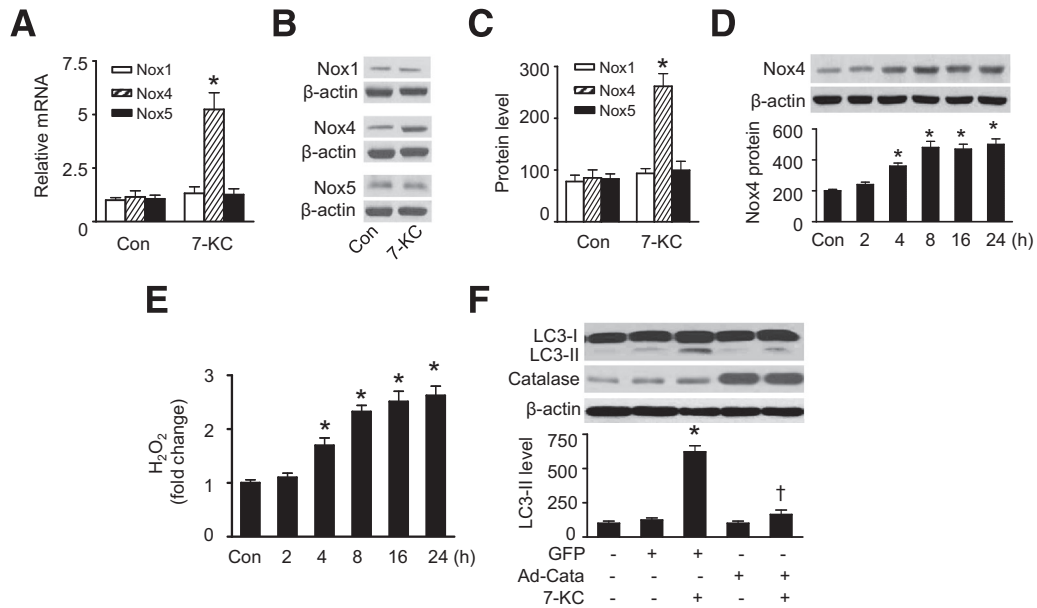


**Figure 2** 7-KC-induced autophagy is mediated by Nox4-derived hydrogen peroxide. **A:** HASMCs were incubated with 20  $\mu\text{mol/L}$  7-KC for 16 hours. The mRNA levels of Nox1, Nox4, and Nox5 were measured by using real-time PCR ( $n = 4$ ).  $*P < 0.05$  versus control (Con). **B and C:** Protein levels of Nox1, Nox4, and Nox5 were determined by using Western blot analysis and quantified by using densitometry ( $n = 4$ ).  $*P < 0.05$  versus Con. **D:** HASMCs were treated with 7-KC (20  $\mu\text{mol/L}$ ) for indicated times. Nox4 protein levels in cell lysates were analyzed by using Western blot analysis (**upper panel**) and quantified by using densitometry (**lower panel**) ( $n = 4$ ).  $P < 0.05$  versus Con. **E:** HASMCs were incubated with 20  $\mu\text{mol/L}$  7-KC for the indicated times, and hydrogen peroxide was detected by using a hydrogen peroxide cell-based assay kit ( $n = 5$ ).  $*P < 0.05$  versus Con. **F:** HASMCs were infected with adenovirus encoding GFP or catalase (Cata) for 48 hours and then incubated with 7-KC (20  $\mu\text{mol/L}$ ) for 16 hours. Protein levels of LC3-II and catalase were detected by using Western blot analysis (**upper panel**) and quantified by using densitometry (**lower panel**) ( $n = 5$ ).  $*P < 0.05$  versus GFP or Con,  $^{\dagger}P < 0.05$  versus GFP/7-KC.

Jose, CA) according to the supplier's instructions. Briefly, HASMCs were collected by using a brief trypsin treatment and were labeled for 15 minutes with Alexa 488-conjugated Annexin V and propidium iodide (PI). Labeled cells were analyzed with FACScan flow cytometry (Becton-Dickinson, Bedford, MA) and CellQuest software (version 5.1; Becton-Dickinson, Bedford, MA).

#### Measurement of Atg4B Activity Using LC3B-PLA 2 Substrate

His-tagged LC3B-PLA2 plasmid was kindly provided by Dr. John C. Reed (Sanford-Burnham Medical Research Institute, La Jolla, CA). The LC3B-PLA2 fusion protein was produced and purified as described.<sup>22</sup> After the treatment, cells were harvested and cell lysates were centrifuged at  $16,000 \times g$  for 15 minutes. The supernatant was used for the LC3B-PLA2 reporter assay to measure Atg4B activity. Briefly, lysates were mixed with 100 nmol/L LC3B-PLA2 fusion protein in 20  $\mu\text{L}$  PLA2 reaction buffer containing 20 mmol/L Tris-HCl, pH 8.0, 2 mmol/L  $\text{CaCl}_2$ , 1 mmol/L DTT, and 20  $\mu\text{mol/L}$  2-(6-(7-nitrobenz-2-oxa-1,3-diazol-4-yl)amino) hexanoyl-1-hexadecanoyl-sn-glycero-3-phosphocholine (NBD-C6-HPC) (N-3786; Invitrogen). Fluorescence intensity was measured within 30 to 60 minutes by using a Bio-Tek Instrument (Winooski, VA) at room temperature with excitation and emission wavelength of 485 and 530, respectively.

#### Statistical Analysis

Quantitative data were presented as the means  $\pm$  SEM. Statistical analyses were performed by using *t*-tests (2 groups) or one-way analysis of variance with the Bonferroni's procedure for multiple comparison tests ( $\geq 3$  groups).  $P < 0.05$  was considered statistically significant.

## Results

### 7-KC Induces Autophagy in HASMCs

To establish whether 7-KC induces autophagy in VSMCs, HASMCs were exposed to 20  $\mu\text{mol/L}$  of 7-KC for up to 24 hours, a concentration comparable to the mean serum level of 7-KC in normal cholesterolemic human subjects (16.9  $\mu\text{mol/L}$ ),<sup>23</sup> and the conversion of LC3-I to LC3-II was then determined. LC3-II protein started to accumulate at 8 hours after treatment and reached a peak at 24 hours (Figure 1A). Next, autophagy induction was measured in HASMCs treated with different concentrations (0 to 40  $\mu\text{mol/L}$ ) of 7-KC. An increase in LC3-II levels was first observed at 10  $\mu\text{mol/L}$  and was elevated to sixfold at 40  $\mu\text{mol/L}$  (Figure 1B). To study the effect of 7-KC on autophagic flux, HASMCs were treated with 7-KC in the presence or absence of 5  $\mu\text{mol/L}$  lysosomal inhibitor CQ. Administration of CQ stimulated LC3-II accumulation. Treatment of cells with both 7-KC and



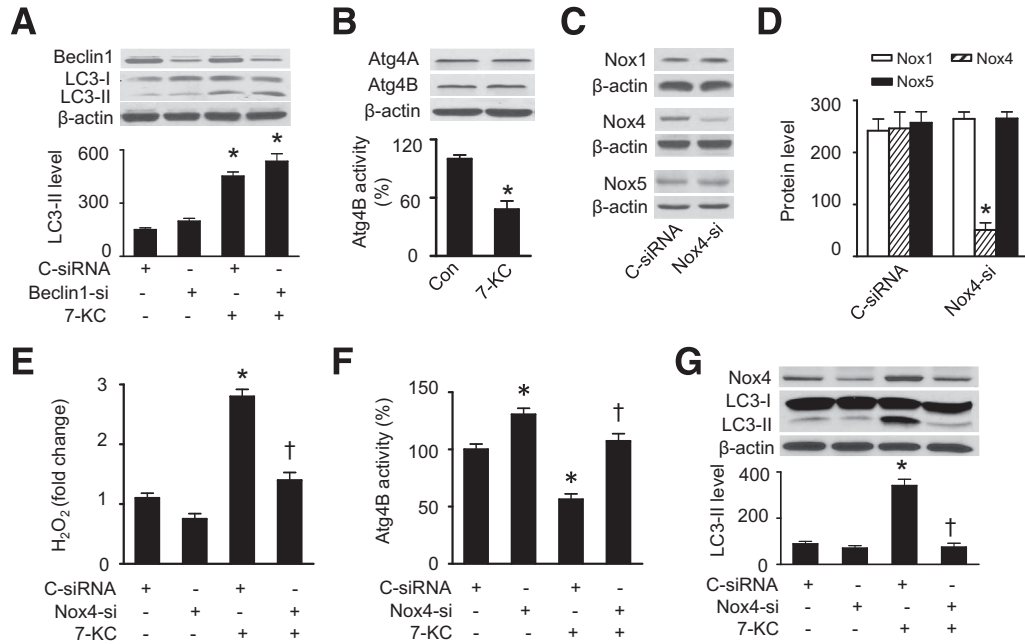


**Figure 3** The 7-KC–stimulated autophagy is mediated by inhibition of Atg4B. HASMCs were transfected with control or Beclin1 siRNA for 48 hours and then treated with 7-KC (20  $\mu$ mol/L) for 16 hours. Expression of Beclin1 and LC3-II were measured by using Western blot analysis (A, upper panel) and quantified by using densitometry (A, lower panel) ( $n = 5$ ). \* $P < 0.05$  versus C-siRNA. HASMCs were treated with 7-KC (20  $\mu$ mol/L) for 16 hours and the expression of Atg4A and Atg4B was measured by using Western blot analysis (B, upper panel). Atg4B activity in cell lysates was assayed as described in *Materials and Methods* (B, lower panel) ( $n = 6$ ). \* $P < 0.05$  versus control (Con). HASMCs were transfected with control or Nox4 siRNA for 48 hours, and protein levels of Nox1, Nox4, and Nox5 were assessed by using Western blot analysis (C) and quantified by using densitometry (D) ( $n = 3$ ). \* $P < 0.05$  versus Con. E: HASMCs were transfected with control or Nox4 siRNA for 48 hours and were then treated with 20  $\mu$ mol/L 7-KC for 16 hours. Hydrogen peroxide was measured by using a hydrogen peroxide cell-based assay kit ( $n = 4$ ). \* $P < 0.05$  versus C-siRNA, † $P < 0.05$  versus C-siRNA/7-KC. F: Atg4B activity in cell lysates was assayed as described in *Materials and Methods* ( $n = 5$ ). \* $P < 0.05$  versus C-siRNA, † $P < 0.05$  versus C-siRNA/7-KC. G: Expression of LC3-II and Nox4 was examined by using Western blot analysis ( $n = 4$ ). \* $P < 0.05$  versus C-siRNA; † $P < 0.05$  versus C-siRNA/7-KC.

CQ induced a further increase in LC3-II protein levels (Figure 1C). Then we performed immunofluorescence analysis in HASMCs expressing GFP-LC3 to confirm the effect of 7-KC on autophagosome formation, because the number of punctate LC3 and GFP-LC3 structures per cell is usually an accurate measure of autophagosome.<sup>24</sup> In the absence of CQ, 7-KC treatment enhanced the number and distribution of GFP-LC3 punctate structures. Addition of CQ induced a further increase in autophagosome formation in the cells treated with 7-KC (Figure 1, D and E). These results indicate that 7-KC acts by inducing autophagosome formation rather than by disrupting its maturation into the autophagolysosome.

### 7-KC–Induced Autophagy Is ROS Dependent

To determine whether ROS mediates 7-KC–induced autophagy, we detected 7-KC–induced autophagy after treating the cells with an ROS scavenger and an antioxidant. Pretreatment of cells with N-acetyl cysteine, which can act both as a precursor for reduced glutathione and as a direct ROS scavenger,<sup>25</sup> attenuated 7-KC–enhanced LC3-II accumulation (Figure 1F). Similarly, administration of apocynin, an antioxidant in the vascular system,<sup>26</sup> depressed 7-KC–elevated LC3-II protein levels (Figure 1G). These data indicate that 7-KC–induced autophagy is ROS-dependent.

### Nox4-Derived Hydrogen Peroxide Mediates 7-KC–Induced Autophagy

NADPH oxidases are major sources of ROS under physiological and pathological conditions.<sup>27</sup> In the vascular system, VSMCs express mainly Nox1, Nox4, and Nox5.<sup>28,29</sup> To verify whether NADPH oxidases contribute to 7-KC–induced ROS production, we assessed the expression of NADPH oxidases in HASMCs exposed to 7-KC. As shown in Figure 2A–C, 7-KC treatment increased expression of Nox4 at mRNA and protein levels, but did not affect mRNA and protein expression of Nox1 and Nox5 (Figure 2A–C). Several recent studies demonstrated that Nox4 generates predominantly hydrogen peroxide rather than superoxide.<sup>30,31</sup> Therefore, we determined whether induction of Nox4 by 7-KC enhanced hydrogen peroxide generation. As expected, the up-regulation of Nox4 protein levels (Figure 2D) was accompanied by higher levels of intracellular hydrogen peroxide (Figure 2E). The increases in Nox4 and hydrogen peroxide occurred before the induction of autophagy, suggesting that Nox4-derived hydrogen peroxide is involved in 7-KC–induced autophagy. Indeed, removal of hydrogen peroxide by overexpression of adenovirus encoding catalase attenuated 7-KC–induced autophagy, whereas transfection of GFP adenovirus failed to diminish autophagy

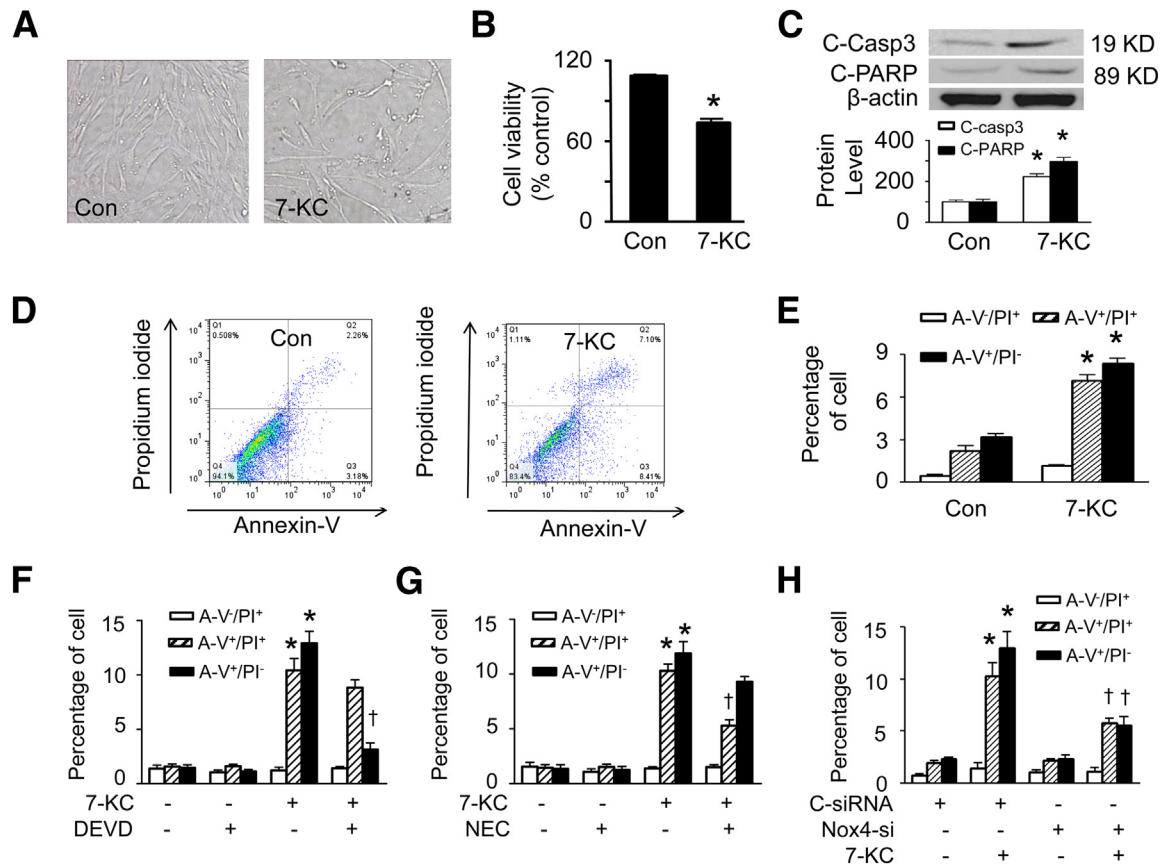


**Figure 4** The 7-KC induces apoptosis and cell death in HASMCs. The HASMCs were treated with 20  $\mu\text{mol/L}$  7-KC for 16 hours. **A:** Morphological changes of HASMCs in response to 7-KC were evaluated under phase contrast microscopy. Similar results were obtained in three independent experiments. **B:** Cell viability was determined by using the cell counting kit-8 ( $n = 4$ ).  $*P < 0.05$  versus control (Con). **C:** Expression of cleaved caspase-3 (C-Casp3) and cleaved poly (ADP-ribose) polymerase (C-PARP) in HASMCs was assessed by using Western blot analysis ( $n = 5$ ).  $*P < 0.05$  versus Con. **D** and **E:** Cell death was analyzed by using annexin V/propidium iodide (PI) staining and flow cytometry ( $n = 4$ ).  $*P < 0.05$  versus Con. **F:** HASMCs were stimulated with 20  $\mu\text{mol/L}$  7-KC for 16 hours after treatment with 20  $\mu\text{mol/L}$  Ac-DEVD-CMK (DEVD) for 30 minutes. Cell death was analyzed by using annexin V/PI staining and flow cytometry ( $n = 5$ ).  $*P < 0.05$  versus C-siRNA,  $\dagger P < 0.05$  versus C-siRNA/7-KC. **G:** HASMCs were pretreated with 40  $\mu\text{mol/L}$  necrostatin (NEC) for 30 minutes and followed by treatment with 20  $\mu\text{mol/L}$  7-KC for 16 hours. Cell death was analyzed by using annexin V/PI staining and flow cytometry ( $n = 5$ ).  $*P < 0.05$  versus Con,  $\dagger P < 0.05$  versus 7-KC. **H:** HASMCs were stimulated with 20  $\mu\text{mol/L}$  7-KC for 16 hours after transfection of control or Nox4 siRNA for 48 hours. Cell death was analyzed by using annexin V/PI staining and flow cytometry ( $n = 5$ ).  $*P < 0.05$  versus C-siRNA,  $\dagger P < 0.05$  versus C-siRNA/7-KC.

induced by 7-KC (Figure 2F). Thus, Nox4-derived hydrogen peroxide was required for 7-KC-induced autophagy.

### Nox4-Derived Hydrogen Peroxide Enhances Autophagy through Inhibition of Atg4B Activity

Currently, more than 30 autophagic-related genes have been identified.<sup>32</sup> Among them Beclin1, the mammalian ortholog of yeast Atg6, is a critical factor required for the initiation of autophagy.<sup>33</sup> First we determined whether Beclin1 participates in the regulation of 7-KC-induced autophagy by transfecting HASMCs with control or Beclin1-specific siRNA. Beclin1 siRNA, but not control siRNA, significantly reduced Beclin1 protein levels. The reduction of Beclin1 expression did not affect 7-KC-induced LC3-II accumulation (Figure 3A), suggesting that Beclin1 may not be involved in 7-KC-induced autophagy. Next we investigated whether Atg4 is involved in 7-KC-induced autophagy because a recent report showed that starvation-induced ROS, specifically hydrogen peroxide, acted

as signaling molecules in autophagy through the inhibition of Atg4 activity and consequently reduced LC3-II delipidation.<sup>8</sup> Although 7-KC did not affect the expression of Atg4A and Atg4B (Figure 3B), it significantly inhibited Atg4B activity (Figure 3B).

To determine whether Nox4-mediated hydrogen peroxide formation contributes to 7-KC-induced autophagy through inhibition of Atg4B activity, we inhibited Nox4 expression by using a gene silencing technique. Compared with control siRNA, Nox4-specific siRNA significantly reduced Nox4 protein levels without affecting the expression of the other related proteins, Nox1 and Nox5 (Figure 3, C and D). Knockdown of Nox4 diminished hydrogen peroxide levels under basal conditions and attenuated 7-KC-enhanced hydrogen peroxide formation (Figure 3E). The reduction of Nox4 concomitantly increased Atg4B activity and prevented 7-KC-inhibited Atg4B activity (Figure 3F). Accordingly, enhanced accumulation of LC3-II protein by 7-KC treatment was suppressed by silencing of the Nox4

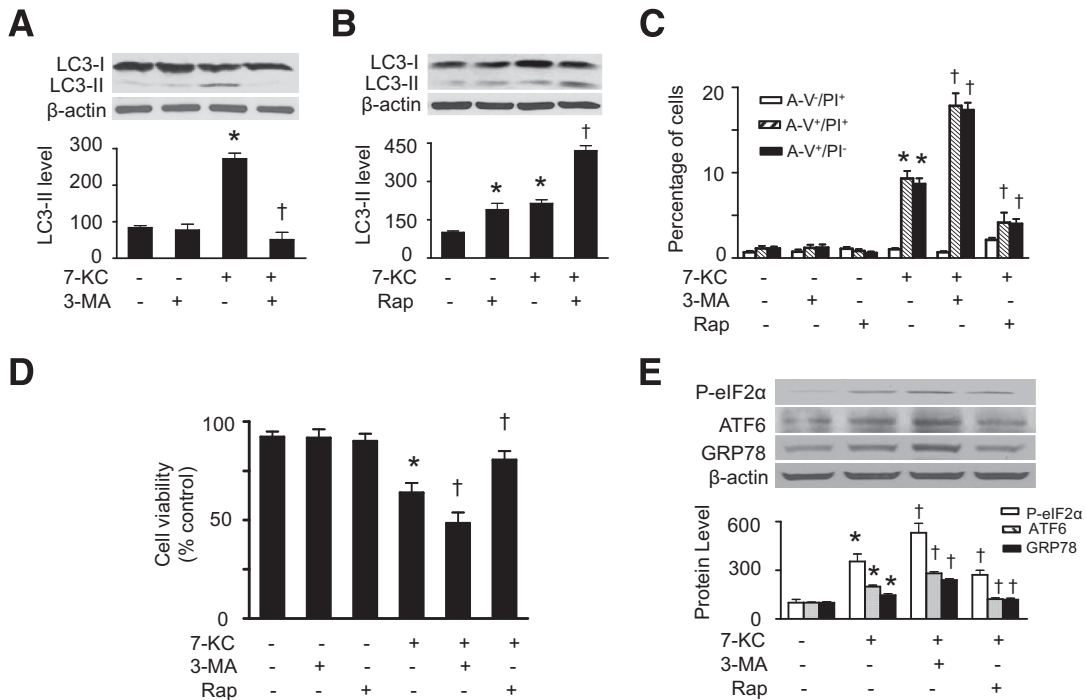


**Figure 5** Effects of autophagy on 7-KC–induced ER stress and cell death. **A** and **B**: HASMCs were pretreated with 3-MA (3 mmol/L) or rapamycin (Rap, 1 μmol/L) for 1 hour and then treated with 7-KC (20 μmol/L) for 16 hours. LC3-II levels in cell lysates were detected by using Western blot analysis (**upper panel**) and quantified by using densitometry (**lower panel**) ( $n = 4$ ). **C**: Cell death was analyzed by using flow cytometry ( $n = 4$ ). **D**: Cell viability was estimated by using the CCK-8 kit ( $n = 4$ ). **E**: HASMCs were pretreated with 3-MA or rapamycin for 1 hour and then treated with 7-KC (20 μmol/L) for 16 hours. The markers of ER stress such as P-eIF2α, ATF6, and GRP78 were detected by using Western blot analysis (**upper panel**) and quantified by using densitometry (**lower panel**) ( $n = 5$ ). \* $P < 0.05$  versus control (Con); † $P < 0.05$  versus 7-KC.

gene (Figure 3G). These findings are consistent with the observation that hydrogen peroxide reduces Atg4 activity, which promotes lipidation of Atg8 (LC-3) and increases autophagic capacity.<sup>8</sup>

### 7-KC Induces Cell Death in VSMCs

To determine the physiological role of 7-KC–induced autophagy, we evaluated the effect of autophagy on cell death in HASMCs. As assessed by inverted phase microscopy, 7-KC treatment was associated with cell rounding and detachment from the plate substrate (Figure 4A). The cell viability was significantly lower in HASMCs exposed to 7-KC than in the control cells (Figure 4B). Western blot analysis showed that administration of 7-KC significantly enhanced the apoptosis markers, such as cleavages of caspase-3 and poly (ADP-ribose) polymerase (Figure 4C), suggesting that 7-KC induces apoptosis. Next, we analyzed the effect of 7-KC on cell death by using annexin V-fluorescein isothiocyanate and PI double labeling and flow cytometry. Early apoptosis with intact membrane (annexin V<sup>+</sup>/PI<sup>-</sup>), end-stage apoptosis and dead cells (annexin V<sup>+</sup>/PI<sup>+</sup>), and damaged cells (annexin V<sup>-</sup>/PI<sup>+</sup>) were distinguished on the basis of double labeling for annexin V-fluorescein isothiocyanate and PI. 7-KC treatment led to dramatic increases in the percentages of apoptotic cells (annexin V<sup>+</sup>/PI<sup>-</sup>) and end-stage apoptosis (annexin V<sup>+</sup>/PI<sup>+</sup>), and to a lesser extent, in the percentage of damaged cells (annexin V<sup>-</sup>/PI<sup>+</sup>) (Figure 4, D and E).

We further analyzed the effect of 7-KC on cell death after treating the cells with either caspase-3 inhibitor, Ac-DEVD-CMK, or the receptor-interacting protein kinase inhibitor, necrostatin. Inhibition of caspase-3 reduced 7-KC–enhanced annexin V<sup>+</sup>/PI<sup>-</sup> cells (Figure 4F), whereas inhibition of receptor interacting protein kinase reduced 7-KC–enhanced annexin V<sup>+</sup>/PI<sup>+</sup> cells (Figure 4G), suggesting that 7-KC induces cell death through enhancing early apoptosis (annexin V<sup>+</sup>/PI<sup>-</sup>), as well as end-stage apoptosis and dead cells (annexin V<sup>+</sup>/PI<sup>+</sup>). To test the role of Nox4 and hydrogen peroxide in 7-KC–induced cell death, HASMCs were transfected with control or Nox4 siRNA and treated with 7-KC. After the treatment, cell death was analyzed by using flow cytometry. As shown in Figure 4H, Nox4 siRNA, which prevented 7-KC–enhanced intracellular hydrogen peroxide levels, reduced apoptotic cells (annexin V<sup>+</sup>/PI<sup>-</sup>) and end-stage apoptosis and dead cells (annexin V<sup>+</sup>/PI<sup>+</sup>) in the 7-KC–treated HASMCs.

### 7-KC–Induced Autophagy Attenuates Cell Death in VSMCs

To determine the relationship between autophagy and cell death during 7-KC treatment, we examined the effects of 7-KC on cell viability and cell death after manipulation of autophagic activity. Administration of 3-methyladenine, a phosphoinositide 3-kinase inhibitor, which suppresses autophagy, attenuated 7-KC–enhanced LC3-II protein levels

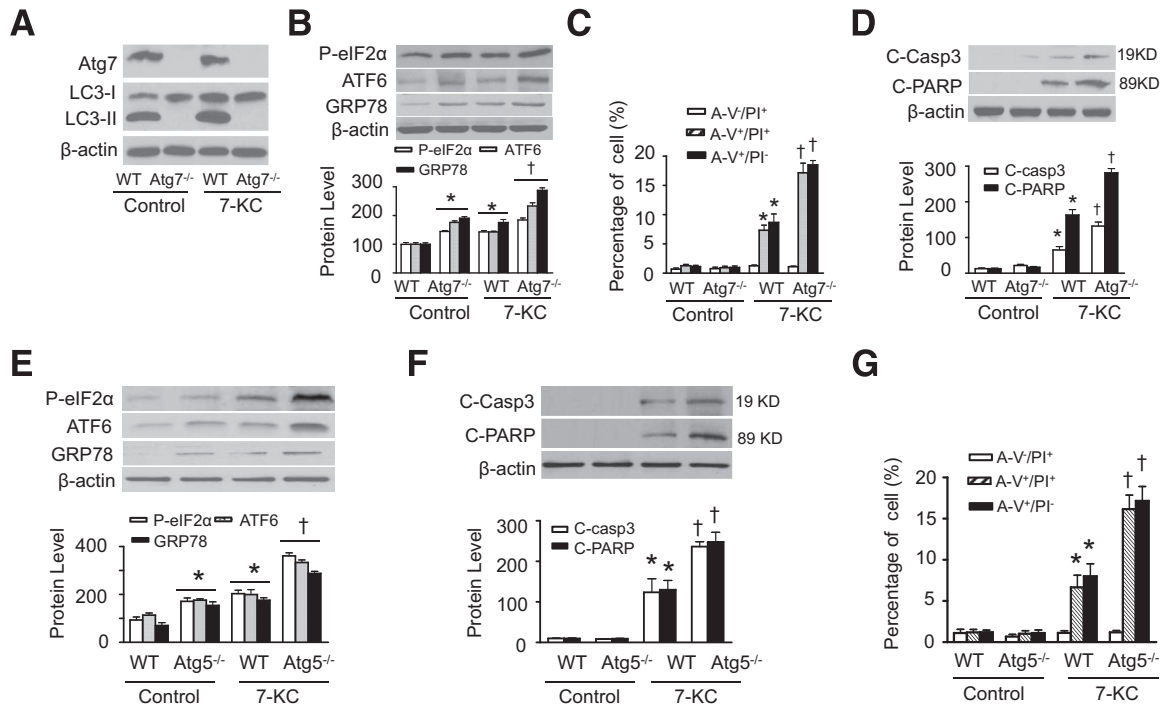


**Figure 6** Deletion of Atg5 or Atg7 aggravates 7-KC–induced ER stress and cell death. Wild-type (WT) and *Atg7*<sup>-/-</sup> MEF were treated with or without 20  $\mu$ mol/L 7-KC for 16 hours and cell lysates were prepared. **A:** The expression of Atg7 and LC3-II were determined by using Western blot analysis ( $n = 5$ ). **B:** ER stress markers including P-eIF2 $\alpha$ , ATF6, and GRP78 were detected by using Western blot analysis (**upper panel**) and quantified by using densitometry (**lower panel**) ( $n = 4$ ). **C:** Cell death was analyzed by using flow cytometry ( $n = 4$ ). **D:** Cleaved caspase-3 (C-Casp3) and cleaved poly (ADP-ribose) polymerase (C-PARP) were detected by using Western blot analysis (**upper panel**) and quantified by using densitometry (**lower panel**) ( $n = 5$ ). **E:** WT and *Atg5*<sup>-/-</sup> MEF were treated with or without 7-KC (20  $\mu$ mol/L) for 16 hours and cell lysates were prepared. ER stress markers including P-eIF2 $\alpha$ , ATF6, and GRP78 were measured by using Western blot analysis (**upper panel**) and quantified by using densitometry (**lower panel**) ( $n = 4$ ). **F:** C-Casp3 and C-PARP were detected by using Western blot analysis (**upper panel**) and quantified by using densitometry (**lower panel**) ( $n = 5$ ). **G:** Cell death was analyzed by using flow cytometry ( $n = 4$ ). \* $P < 0.05$  versus wild-type (WT)/Control, † $P < 0.05$  versus WT/7-KC.

(Figure 5A), whereas treatment of cells with rapamycin, an inhibitor of the mammalian target of rapamycin,<sup>34</sup> which enhances autophagy, aggravated 7-KC–induced accumulation of LC3-II protein (Figure 5B). Notably, the inhibition of autophagy by 3-methyladenine exacerbated 7-KC–induced cell death, as indicated by reduced cell viability and increased cell death (including annexin V<sup>+</sup>/PI<sup>-</sup> cells and annexin V<sup>+</sup>/PI<sup>+</sup> cells) (Figure 5, C and D). Conversely, induction of autophagy by rapamycin improved cell viability and mitigated 7-KC–enhanced annexin V<sup>+</sup>/PI<sup>-</sup> cells and annexin V<sup>+</sup>/PI<sup>+</sup> cells (Figure 5, C and D).

Recent work suggests a bidirectional regulation exists between autophagy and ER stress,<sup>35</sup> an important signaling in the regulation of apoptosis.<sup>36</sup> Therefore, we studied whether 7-KC–induced autophagy attenuates apoptosis through regulation of ER stress. As shown in Figure 5E, incubation of HASMCs with 7-KC increased expression of ER stress markers, including P-eIF2 $\alpha$ , activating transcription factor 6, and GRP78. The pretreatment of cells with 3-methyladenine to inhibit autophagy exaggerated the 7-KC–induced ER stress. Conversely, enhanced autophagy by rapamycin attenuated ER stress. These data suggest that 7-KC–induced autophagy in HASMCs may attenuate cell death through inhibition of ER stress.

### Genetic Inhibition of Autophagy Aggravates 7-KC–Induced ER Stress and Cell Death

We further determined the effect of 7-KC–induced autophagy on cell death in wild-type, *Atg5*<sup>-/-</sup>, and *Atg7*-deficient (*Atg7*<sup>-/-</sup>) mouse embryonic fibroblast [MEFs; a gift from Dr. Noboru Mizushima (Japan Science and Technology Agency, Tokyo, Japan)<sup>37</sup> and Masaaki Komatsu (Tokyo Metropolitan Institute of Medical Science, Tokyo, Japan)<sup>38</sup>]. The deletion of *Atg7* completely prevented the conversion of LC3-I to LC3-II under basal conditions and abolished LC3-II accumulation in response to 7-KC (Figure 6A), suggesting that autophagy is suppressed. Inhibition of autophagy resulted in higher expression of ER stress markers in *Atg7*<sup>-/-</sup> MEFs than in wild-type MEFs under basal conditions. In addition, ER stress was aggravated when *Atg7*<sup>-/-</sup> MEFs were treated with 7-KC (Figure 6B). As a result, inhibition of autophagy exacerbated 7-KC–induced cell death in *Atg7*<sup>-/-</sup> MEFs, as evidenced by more annexin V<sup>+</sup>/PI<sup>-</sup> and annexin V<sup>+</sup>/PI<sup>+</sup> cells (Figure 6C) and the higher levels of the cleavage products of caspase 3 and poly (ADP-ribose) polymerase (Figure 6D).

Similar to the observations in *Atg7*<sup>-/-</sup> MEFs, deletion of *Atg5* also increased ER stress markers, including P-eIF2 $\alpha$ ,



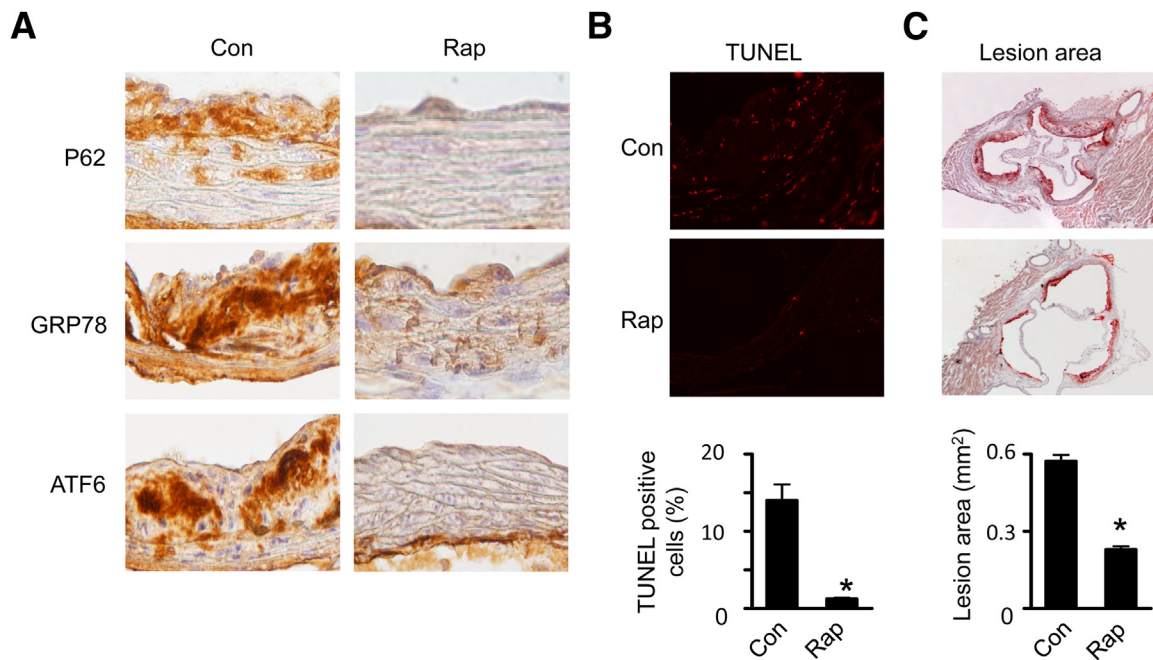


**Figure 7** Effects of rapamycin on ER stress and apoptosis in *ApoE*<sup>-/-</sup> mice. **A:** Aortas isolated from *ApoE*<sup>-/-</sup> mice treated with or without rapamycin (Rap) were sectioned, and the expression of P62, GRP78, and activating transcription factor 6 (ATF6) was detected by using immunohistochemistry with specific antibodies. Three samples in each group were analyzed and showed similar results. **B:** Representative images of TUNEL staining in aortas from control (Con) and Rap-treated *ApoE*<sup>-/-</sup> mice. The number of TUNEL-positive cells is shown in the bar graph ( $n = 6$  per group). **C:** Atherosclerotic lesion size in the aortic root was determined by Oil Red O staining ( $n = 6$  per group). \* $P < 0.05$  versus Con.

activating transcription factor 6, and GRP78 under basal conditions and aggravated 7-KC-induced ER stress and cell death (including annexin V<sup>+</sup>/PI<sup>-</sup> and annexin V<sup>+</sup>/PI<sup>+</sup> cells) in *Atg5*<sup>-/-</sup> MEFs (Figure 6, E and F). These observations indicate that defective autophagy aggravates 7-KC-triggered ER stress and cell death.

#### Activation of Autophagy by Rapamycin Attenuates ER Stress, Apoptosis, and Atherosclerosis in *ApoE*<sup>-/-</sup> Mouse Aortas

To extend our *in vitro* findings, we used *ApoE*<sup>-/-</sup> mice, a well-characterized animal model of atherosclerosis, to investigate the effect of rapamycin on ER stress, apoptosis, and atherosclerotic lesion areas. Two weeks of rapamycin treatment reduced the autophagic substrate P62 protein levels (Figure 7A), suggesting that autophagy was activated. Also, immunohistochemical analysis demonstrated that ER stress markers, such as GRP78 and activating transcription factor 6, were lower in these mice (Figure 7A). The effect of up-regulation of autophagy on apoptosis was evaluated by using the TUNEL technique. As depicted in Figure 7B, fewer TUNEL-positive cells were observed in rapamycin-treated aortas. Quantitative analysis validated the presence of fewer TUNEL-positive cells in rapamycin-treated *ApoE*<sup>-/-</sup> mice. We further examined the impact of activation of autophagy on atherogenesis by using Oil Red O staining and found that chronic administration of rapamycin significantly reduced atherosclerotic lesion area in the *ApoE*<sup>-/-</sup> mice (Figure 7C).

#### Discussion

The increased production of ROS has been implicated in various pathological conditions, including ischemic injury, diabetes, and atherosclerosis. ROS, originally considered to cause cell damage, are now recognized to be signaling molecules that mediate diverse biological responses, such as the activation of transcriptional factors and the phosphorylation of kinases.<sup>39</sup> In the present study, 7-KC-induced autophagy was suppressed by administration of ROS scavenger N-acetyl cysteine<sup>25</sup> and vascular system antioxidant apocynin,<sup>26</sup> supporting the hypothesis that 7-KC up-regulates autophagy through increasing ROS generation.

NADPH oxidases are the primary enzymes responsible for inducible ROS formation in the vascular system. Under physiological conditions, NADPH oxidases produce ROS at levels that serve as signaling molecules in a variety of intracellular processes. However, under pathological conditions, NADPH oxidases become overexpressed and generate excess ROS. The increased amount of ROS leads to endothelial dysfunction, inflammation, and vascular remodeling. In HASMCs, the administration of 7-KC increased Nox4 protein and intracellular hydrogen peroxide levels leading to the inhibition of Atg4B activity. Transfection of cells with adenovirus encoding catalase to remove hydrogen peroxide prevented 7-KC-induced autophagy. Moreover, gene silencing of Nox4 reduced intracellular hydrogen peroxide levels, restored Atg4B activity, and attenuated 7-KC-induced autophagy. Thus, Nox4-derived hydrogen peroxide may serve as a signaling molecule to induce autophagy in response to 7-KC treatment.

Under starvation conditions, enhanced hydrogen peroxide triggers autophagy through modulating Atg4 activity.<sup>8</sup> Atg4s are cysteine proteases that have several conserved cysteine residues.<sup>40</sup> In mammals, at least four Atg4 homologues have been reported.<sup>40</sup> Atg4 cleaves Atg8 (LC3) near its C-terminal arginine residue, and the exposed C-terminal glycine is conjugated to phosphatidylethanolamine by an ubiquitin-like system. This conjugate (Atg8–phosphatidylethanolamine) incorporates into the autophagosomal membrane and plays a crucial role in autophagosome formation.<sup>41</sup> On the other hand, Atg4 also delipidates Atg8, leading to the release of Atg8 from the autophagosomal membrane and the disassembly of the autophagosome.<sup>42</sup> Hence, the inactivation of Atg4 after the initial cleavage of Atg8 is essential for the conjugation of Atg8 to the autophagosomal membrane, which ensures the structural integrity of the mature autophagosome, thereby promoting autophagy.

Recently, Scherz-Shouval et al<sup>8</sup> have found that ROS are involved in starvation-induced autophagy as signaling molecules, and have identified both cysteine residue 81 in Atg4A and cysteine residue 78 in Atg4B are redox regulated in this process. They concluded that the delipidation activity of Atg4 is the main target of this regulation.<sup>8</sup> In our system, 7-KC enhanced intracellular hydrogen peroxide, reduced Atg4B activity, and increased autophagic capacity. Knockdown of Nox4 attenuated 7-KC–enhanced intracellular hydrogen peroxide and restored Atg4B activity, which mitigated 7-KC–induced autophagy. These observations indicate that 7-KC may enhance intracellular hydrogen peroxide through up-regulation of Nox4. This leads to the oxidation and inhibition of Atg4B, ultimately promoting lipidation of Atg8 (LC3) and enhancing autophagy. The specific molecular mechanisms underlying these processes require additional investigation.

Oxidized lipids have been reported to stimulate autophagy in advanced human atherosclerotic plaques and in cultured VSMCs.<sup>43</sup> For instance, in experimental and human plaques, VSMCs exhibit the characteristics of autophagy, such as the formation of myelin figure and severe vacuolization.<sup>11</sup> Death-associated protein kinase, a positive mediator of autophagic vacuole formation, is up-regulated in lipid-laden smooth muscle cells in human plaques.<sup>44</sup> Moreover, 4-hydroxynonenal, a lipid peroxidation product, activates autophagy in rat aortic smooth muscle cells.<sup>45</sup> In the present study, we observed autophagy and apoptosis in 7-KC–treated HASMCs, suggesting that cross talk occurs between these two important cellular processes in the development of atherosclerosis. These data are consistent with previous findings that 7-KC triggers oxidative stress, up-regulates autophagic genes,<sup>46</sup> and promotes conversion of LC3-I to LC3-II in smooth muscle cells,<sup>12,47</sup> in addition to inducing apoptosis.

However, whether induction of autophagy in VSMCs exposed to 7-KC is the cause of death or it is actually an attempt to support survival in response to cellular stress remains to be determined. Interestingly, Martinet et al<sup>47</sup> reported that 7-KC–induced autophagy attenuated statin-

induced VSMC apoptosis through interfering with caspase activation. An additional study shows that macrophage autophagy plays a protective role in advanced atherosclerosis.<sup>48</sup> In our model system, inhibition of autophagy by the administration of 3-methyladenine in HASMCs and deletion of Atg5 or Atg7 in mouse embryonic fibroblasts enhanced ER stress and cell death in the cells treated with 7-KC. Conversely, up-regulation of autophagic activity by rapamycin inhibited 7-KC–induced ER stress and cell death. These findings suggest that increased autophagy in response to 7-KC may be an adaptive survival strategy that recycles cellular components for intermediary metabolism and eliminates damaged organelles, such as mitochondria,<sup>49</sup> thereby protecting against ER stress and apoptotic cell death. This conclusion is further supported by our *in vivo* studies that show the up-regulation of autophagy by chronic administration of rapamycin was associated with the suppression of ER stress, apoptosis, and atherosclerosis in *ApoE*<sup>−/−</sup> mouse aortas.

Rabbits have been extensively used for the experimental production of arterial lesions by cholesterol feeding. In sharp contrast to human atherosclerotic lesions, the rabbit lesions are composed principally of foam cells and have seldom developed necrosis and complications such as calcification, ulceration, and thrombosis.<sup>50</sup> Mitochondrial stress is induced by 7-KC, which leads to autophagic cell death in rabbit aorta smooth muscle cells.<sup>47</sup> However, 7-KC–induced autophagy in HASMCs seems to be protective. This type of tissue reaction suggests that the arteries of rabbits respond to cholesterol in a different manner than that of human arteries.<sup>50</sup>

In summary, our results demonstrate that 7-KC enhanced Nox4-mediated hydrogen peroxide formation, which stimulated autophagy through inhibition of Atg4B activity. In 7-KC–treated HASMCs, suppression of autophagy exaggerated 7-KC–induced ER stress and cell death. Conversely, up-regulation of autophagy mitigated ER stress and cell death induced by 7-KC. Furthermore, chronic rapamycin treatment attenuated ER stress, apoptosis, and atherosclerosis in *ApoE*<sup>−/−</sup> mouse aortas. These findings suggest that activation of autophagy is a beneficial adaptive response that suppresses ER stress and attenuates 7-KC–induced cell death.

## Acknowledgment

We thank Dr. Ming-Hui Zou for helpful discussion.

## References

1. Klionsky DJ: Autophagy: from phenomenology to molecular understanding in less than a decade. *Nat Rev Mol Cell Biol* 2007, 8: 931–937
2. Yang Y, Fukui K, Koike T, Zheng X: Induction of autophagy in neurite degeneration of mouse superior cervical ganglion neurons. *Eur J Neurosci* 2007, 26:2979–2988
3. Xie Z, Lau K, Eby B, Lozano P, He C, Pennington B, Li H, Rathi S, Dong Y, Tian R, Kem D, Zou MH: Improvement of cardiac functions by chronic metformin treatment is associated with enhanced cardiac autophagy in diabetic OVE26 mice. *Diabetes* 2011, 60:1770–1778

4. Zou MH, Xie Z: Regulation of interplay between autophagy and apoptosis in the diabetic heart: new role of AMPK. *Autophagy* 2013, 9:624–625
5. Xie Z, He C, Zou MH: AMP-activated protein kinase modulates cardiac autophagy in diabetic cardiomyopathy. *Autophagy* 2011, 7:1254–1255
6. Martinet W, De Meyer GR: Autophagy in atherosclerosis: a cell survival and death phenomenon with therapeutic potential. *Circ Res* 2009, 104:304–317
7. Stocker R, Kearney JF Jr: Role of oxidative modifications in atherosclerosis. *Physiol Rev* 2004, 84:1381–1478
8. Scherz-Shouval R, Shvets E, Fass E, Shorer H, Gil L, Elazar Z: Reactive oxygen species are essential for autophagy and specifically regulate the activity of Atg4. *EMBO J* 2007, 26:1749–1760
9. Chatterjee S: Role of oxidized human plasma low density lipoproteins in atherosclerosis: effects on smooth muscle cell proliferation. *Mol Cell Biochem* 1992, 111:143–147
10. Brown AJ, Jessup W: Oxysterols and atherosclerosis. *Atherosclerosis* 1999, 142:1–28
11. Martinet W, De BM, Schrijvers DM, De Meyer GR, Herman AG, Kockx MM: 7-ketocholesterol induces protein ubiquitination, myelin figure formation, and light chain 3 processing in vascular smooth muscle cells. *Arterioscler Thromb Vasc Biol* 2004, 24:2296–2301
12. Ghelli A, Porcelli AM, Zanna C, Rugolo M: 7-Ketocholesterol and staurosporine induce opposite changes in intracellular pH, associated with distinct types of cell death in ECV304 cells. *Arch Biochem Biophys* 2002, 402:208–217
13. Miguet-Alfonsi C, Prunet C, Monier S, Bessede G, Lemaire-Ewing S, Berthier A, Menetrier F, Neel D, Gambert P, Lizard G: Analysis of oxidative processes and of myelin figures formation before and after the loss of mitochondrial transmembrane potential during 7 $\beta$ -hydroxycholesterol and 7-ketocholesterol-induced apoptosis: comparison with various pro-apoptotic chemicals. *Biochem Pharmacol* 2002, 64:527–541
14. Xie Z, Dong Y, Zhang J, Scholz R, Neumann D, Zou MH: Identification of the serine 307 of LKB1 as a novel phosphorylation site essential for its nucleocytoplasmic transport and endothelial cell angiogenesis. *Mol Cell Biol* 2009, 29:3582–3596
15. Xie Z, Dong Y, Scholz R, Neumann D, Zou MH: Phosphorylation of LKB1 at serine 428 by protein kinase C-zeta is required for metformin-enhanced activation of the AMP-activated protein kinase in endothelial cells. *Circulation* 2008, 117:952–962
16. Tedesco L, Valerio A, Cervino C, Cardile A, Pagano C, Vettor R, Pasquali R, Carruba MO, Marsicano G, Lutz B, Pagotto U, Nisoli E: Cannabinoid type 1 receptor blockade promotes mitochondrial biogenesis through endothelial nitric oxide synthase expression in white adipocytes. *Diabetes* 2008, 57:2028–2036
17. Pfaffl MW: A new mathematical model for relative quantification in real-time RT-PCR. *Nucleic Acids Res* 2001, 29:e45
18. He C, Zhu H, Li H, Zou MH, Xie Z: Dissociation of Bcl-2-Beclin1 complex by activated AMPK enhances cardiac autophagy and protects against cardiomyocyte apoptosis in diabetes. *Diabetes* 2013, 62:1270–1281
19. He C, Choi HC, Xie Z: Enhanced tyrosine nitration of prostacyclin synthase is associated with increased inflammation in atherosclerotic carotid arteries from type 2 diabetic patients. *Am J Pathol* 2010, 176:2542–2549
20. Li H, Xu M, Lee J, He C, Xie Z: Leucine supplementation increases SIRT1 expression and prevents mitochondrial dysfunction and metabolic disorders in high-fat diet-induced obese mice. *Am J Physiol Endocrinol Metab* 2012, 303:E1234–E1244
21. Zhou M, Diwu Z, Panchuk-Voloshina N, Haugland RP: A stable nonfluorescent derivative of resorufin for the fluorometric determination of trace hydrogen peroxide: applications in detecting the activity of phagocyte NADPH oxidase and other oxidases. *Anal Biochem* 1997, 253:162–168
22. Shu CW, Drag M, Bekes M, Zhai D, Salvesen GS, Reed JC: Synthetic substrates for measuring activity of autophagy proteases: autophagins (Atg4). *Autophagy* 2010, 6:936–947
23. Schroepfer GJ Jr: Oxysterols: modulators of cholesterol metabolism and other processes. *Physiol Rev* 2000, 80:361–554
24. Mizushima N, Yoshimori T, Levine B: Methods in mammalian autophagy research. *Cell* 2010, 140:313–326
25. de GR, Tintu A, Stassen F, Kloppenburg G, Bruggeman C, Rouwet E: N-acetylcysteine prevents neointima formation in experimental venous bypass grafts. *Br J Surg* 2009, 96:941–950
26. Heumuller S, Wind S, Barbosa-Sicard E, Schmidt HH, Busse R, Schroder K, Brandes RP: Apocynin is not an inhibitor of vascular NADPH oxidases but an antioxidant. *Hypertension* 2008, 51:211–217
27. Bedard K, Krause KH: The NOX family of ROS-generating NADPH oxidases: physiology and pathophysiology. *Physiol Rev* 2007, 87:245–313
28. Lassegue B, Sorescu D, Szocs K, Yin Q, Akers M, Zhang Y, Grant SL, Lambeth JD, Griendling KK: Novel gp91(phox) homologues in vascular smooth muscle cells: nox1 mediates angiotensin II-induced superoxide formation and redox-sensitive signaling pathways. *Circ Res* 2001, 88:888–894
29. Pedruzzi E, Guichard C, Ollivier V, Driss F, Fay M, Prunet C, Marie JC, Pouzet C, Samadi M, Elbim C, O'dowd Y, Bens M, Vandewalle A, Gougerot-Pocidallo MA, Lizard G, Ogier-Denis E: NAD(P)H oxidase Nox-4 mediates 7-ketocholesterol-induced endoplasmic reticulum stress and apoptosis in human aortic smooth muscle cells. *Mol Cell Biol* 2004, 24:10703–10717
30. Dikalov SI, Dikalova AE, Bikineyeva AT, Schmidt HH, Harrison DG, Griendling KK: Distinct roles of Nox1 and Nox4 in basal and angiotensin II-stimulated superoxide and hydrogen peroxide production. *Free Radic Biol Med* 2008, 45:1340–1351
31. Schroder K, Zhang M, Benkhoff S, Mieth A, Pliquett R, Kosowski J, Kruse C, Luedike P, Michaelis UR, Weissmann N, Dimmeler S, Shah AM, Brandes RP: Nox4 is a protective reactive oxygen species generating vascular NADPH oxidase. *Circ Res* 2012, 110:1217–1225
32. Klionsky DJ, Cregg JM, Dunn WA Jr, Emr SD, Sakai Y, Sandoval IV, Sibirny A, Subramani S, Thumm M, Veenhuis M, Ohsumi Y: A unified nomenclature for yeast autophagy-related genes. *Dev Cell* 2003, 5:539–545
33. Liang XH, Kleeman LK, Jiang HH, Gordon G, Goldman JE, Berry G, Herman B, Levine B: Protection against fatal Sindbis virus encephalitis by beclin, a novel Bcl-2-interacting protein. *J Virol* 1998, 72:8586–8596
34. Zhang L, Yu J, Pan H, Hu P, Hao Y, Cai W, Zhu H, Yu AD, Xie X, Ma D, Yuan J: Small molecule regulators of autophagy identified by an image-based high-throughput screen. *Proc Natl Acad Sci USA* 2007, 104:19023–19028
35. Hoyer-Hansen M, Jaattela M: Connecting endoplasmic reticulum stress to autophagy by unfolded protein response and calcium. *Cell Death Differ* 2007, 14:1576–1582
36. Schroder M, Kaufman RJ: The mammalian unfolded protein response. *Annu Rev Biochem* 2005, 74:739–789
37. Kuma A, Hatano M, Matsui M, Yamamoto A, Nakaya H, Yoshimori T, Ohsumi Y, Tokuhisa T, Mizushima N: The role of autophagy during the early neonatal starvation period. *Nature* 2004, 432:1032–1036
38. Komatsu M, Waguri S, Ueno T, Iwata J, Murata S, Tanida I, Ezaki J, Mizushima N, Ohsumi Y, Uchiyama Y, Kominami E, Tanaka K, Chiba T: Impairment of starvation-induced and constitutive autophagy in Atg7-deficient mice. *J Cell Biol* 2005, 169:425–434
39. Touyz RM, Briones AM: Reactive oxygen species and vascular biology: implications in human hypertension. *Hypertens Res* 2011, 34:5–14
40. Marino G, Uria JA, Puente XS, Quesada V, Bordallo J, Lopez-Otin C: Human autophagins, a family of cysteine proteinases

- potentially implicated in cell degradation by autophagy. *J Biol Chem* 2003, 278:3671–3678
41. Ichimura Y, Kirisako T, Takao T, Satomi Y, Shimonishi Y, Ishihara N, Mizushima N, Tanida I, Kominami E, Ohsumi M, Noda T, Ohsumi Y: A ubiquitin-like system mediates protein lipidation. *Nature* 2000, 408:488–492
  42. Kirisako T, Ichimura Y, Okada H, Kabeya Y, Mizushima N, Yoshimori T, Ohsumi M, Takao T, Noda T, Ohsumi Y: The reversible modification regulates the membrane-binding state of Apg8/Aut7 essential for autophagy and the cytoplasm to vacuole targeting pathway. *J Cell Biol* 2000, 151:263–276
  43. Martinet W, Knaapen MW, Kockx MM, De Meyer GR: Autophagy in cardiovascular disease. *Trends Mol Med* 2007, 13:482–491
  44. Inbal B, Bialik S, Sabanay I, Shani G, Kimchi A: DAP kinase and DRP-1 mediate membrane blebbing and the formation of autophagic vesicles during programmed cell death. *J Cell Biol* 2002, 157:455–468
  45. Hill BG, Habertzell P, Ahmed Y, Srivastava S, Bhatnagar A: Unsaturated lipid peroxidation-derived aldehydes activate autophagy in vascular smooth-muscle cells. *Biochem J* 2008, 410:525–534
  46. Jia G, Cheng G, Agrawal DK: Autophagy of vascular smooth muscle cells in atherosclerotic lesions. *Autophagy* 2007, 3:63–64
  47. Martinet W, Schrijvers DM, Timmermans JP, Bult H: Interactions between cell death induced by statins and 7-ketocholesterol in rabbit aorta smooth muscle cells. *Br J Pharmacol* 2008, 154:1236–1246
  48. Liao X, Sluimer JC, Wang Y, Subramanian M, Brown K, Pattison JS, Robbins J, Martinez J, Tabas I: Macrophage autophagy plays a protective role in advanced atherosclerosis. *Cell Metab* 2012, 15:545–553
  49. Debnath J, Baehrecke EH, Kroemer G: Does autophagy contribute to cell death? *Autophagy* 2005, 1:66–74
  50. Imai H, Lee KT, Pastori S, Panlilio E, Florentin R, Thomas WA: Atherosclerosis in rabbits. Architectural and subcellular alterations of smooth muscle cells of aortas in response to hyperlipemia. *Exp Mol Pathol* 1966, 5:273–310